2021

Prediction of Fin Efficiency, Air Side Heat Transfer Coefficient, and Air Side Pressure Drop of Flat Tube Heat Exchanger

Akira Yatsuyanagi
Living Environment Systems Laboratory, Mitsubishi Electric Corporation, Shizuoka-City, Shizuoka, Japan, Yatsuyanagi.Akira@ay.MitsubishiElectric.co.jp

Akira Ishibashi

Shin Nakamura

Prediction of Fin Efficiency, Air Side Heat Transfer Coefficient, and Air Side Pressure Drop of Flat Tube Heat Exchanger

Akira YATSUYANAGI[1]*, Akira ISHIBASHI[1] and Shin NAKAMURA[1]

[1] Living Environment Systems Laboratory, Mitsubishi Electric Shizuoka Works, Oshika, Suruga-Ku, Shizuoka-City, Shizuoka, 422-8528, Japan
Phone: +81-54-287-3053, E-mail: Yatsuyanagi.Akira@ay.MitsubishiElectric.co.jp

ABSTRACT

Heat exchangers equipped with circular tubes are generally used in air conditioners. Recently, air conditioners using heat exchangers equipped with flat tubes for higher performance have been enlarging. It is also effective for increasing the efficiency of the air conditioner to improve the performance by optimal design of the heat exchanger. Therefore, it is important to improve the accuracy of the air side performance prediction method. In this study, we propose a new method to predict air side heat transfer characteristics and air side pressure drop characteristics of the flat tube heat exchanger using the numerical analysis.
The calculation results, using a new fin efficiency equation with corrections in the row pitch direction and the column pitch direction, agree well with the numerical analysis results taking into account the air side local heat transfer coefficient. In addition, the calculation results, using non-dimensional equations for the air side heat transfer coefficient and the air side pressure drop under dry conditions in conventional form, and a new fin efficiency equation, agree well with the numerical analysis results and the measurement results. Furthermore, in wet conditions, it is suggested that the existence of the slit has a significant effect on the water film thickness around the pipe back-calculated from the measurement results and the non-dimensional equation.

1. INTRODUCTION

Heat exchangers equipped with circular tubes are generally used in air conditioners. It is effective for increasing the efficiency of the air conditioner to improve the performance by optimal design of the heat exchanger. Especially, it is important to improve the accuracy of the air side performance prediction method. To date, Seshimo *et al*. (1987) proposed unified non-dimensional equations for the air side heat transfer coefficient and the air side pressure drop, and Kondo *et al*. (2006) proposed correction equations improving the prediction accuracy for the heat exchanger equipped with circular tubes, based on non-dimensional equations as mentioned above, using the numerical analysis. Recently, air conditioners using heat exchangers equipped with flat tubes for higher performance have been enlarging. However, there are few studies that propose the method to predict air side heat transfer characteristics and air side pressure drop characteristics of the flat tube heat exchanger.
In this study, we propose a new method to predict air side heat transfer characteristics and air side pressure drop characteristics of the flat tube heat exchanger using the numerical analysis.

2. Dimensions of the flat tube heat exchanger

In the flat tube heat exchanger, fins have notches at one side in the direction of airflow, flat tubes inserted into notches, and flat tubes are arranged in a grid pattern. In this type of the heat exchanger, the condensed water generated in the case of the evaporator and the molten water generated during defrost are drained at the area extending along the longitudinal direction of fins. Figure 1 shows dimensions of the two-row flat tube heat exchanger.

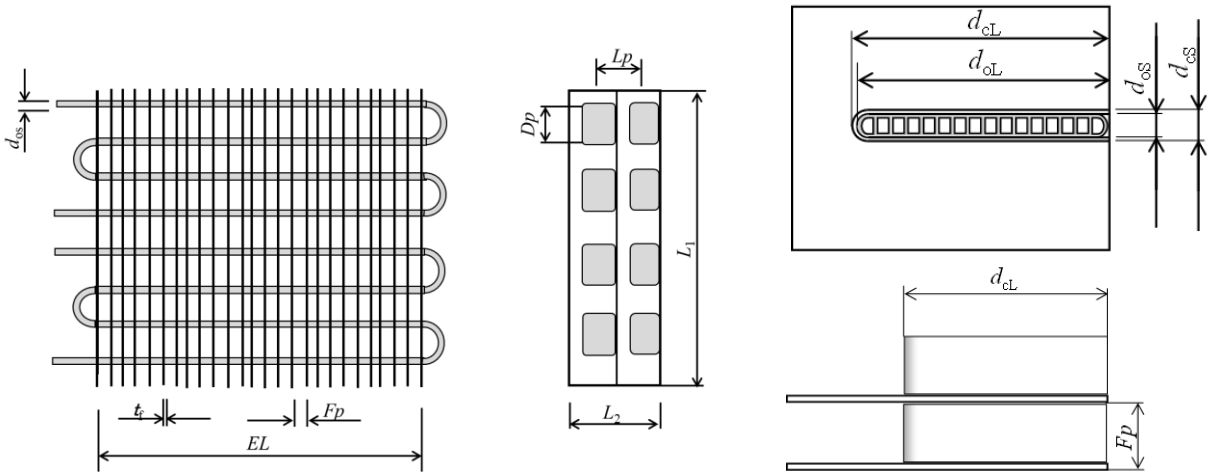

(a) Appearance (b) Details

Figure 1: Specifications of cross fin-tube heat exchanger

3. Fin efficiency

Fujikake (1980) proposed the following equation about the fin efficiency η_f considering the two-dimensional thermal conduction in fins based on the fin efficiency considering the one-dimensional thermal conduction in fins, on the premise that the air side local heat transfer coefficient is constant.

$$\eta_f = \frac{\tanh\beta}{\beta} \tag{1}$$

$$\beta = \frac{Dp - d_{cS}}{2} \cdot \sqrt{\frac{Lp \cdot (Dp - d_{cS}) + d_{cS} \cdot (Lp - d_{cL})}{(d_{cS}/2 + d_{cL}) \cdot (Dp - d_{cS})} \cdot m} \tag{2}$$

$$m = \frac{2h_a}{\lambda_f t_f} \tag{3}$$

In this study, considering the actual air side local heat transfer coefficient, the fin efficiency η_f is arranged by the following equation with corrections in the row pitch direction and the column pitch direction.

$$\beta = \frac{Dp \cdot D_f^{n1}}{2} \cdot \sqrt{\frac{Lp \cdot Dp \cdot D_f^{n1} + d_{cS} \cdot Lp \cdot L_f^{n2}}{(d_{cS}/2 + d_{cL}) \cdot Dp \cdot D_f^{n1}} \cdot m} \tag{4}$$

$$D_f = \frac{Dp - d_{cS}}{Dp}, \qquad n1 = -1.43 \tag{5}$$

$$L_f = \frac{Lp - d_{cL}}{Lp}, \qquad n2 = 1.1 \tag{6}$$

Figure 2 shows the results of comparing the fin efficiency calculated by the above equation (2) and equation (4) with the fin efficiencies obtained by three-dimensional thermal fluid analysis under forced convection conditions. In Table 1, dimensions used in this calculation and analysis are summarized. The calculation result of the fin efficiency by equation (2) was +14% larger than that of numerical analysis, which had large deviation. On the other hand, the calculation result of the fin efficiency by equation (4) was within ±8% of the numerical analysis result, which was in good agreement. This is because equation (4) considers the distribution of the air side local heat transfer coefficient, while equation (2) assumes that the air side local heat transfer coefficient is constant.

Table 1: Range of calculation parameter

Short Side Length of Flat Tube	Long Side Length of Flat Tube	Pipe Pitch		Fin Pitch	Fin Thickness	Frontal Air velocity	Thermal Conductivity of Fin
d_{cS}	d_{cL}	Dp	Lp	Fp	t_f	U_f	λ_f
mm	mm	mm	mm	mm	mm	m/s	W/mK
1.5	10～19	9.5～21.5	15～29	1.6	0.115	1.0～4.0	160

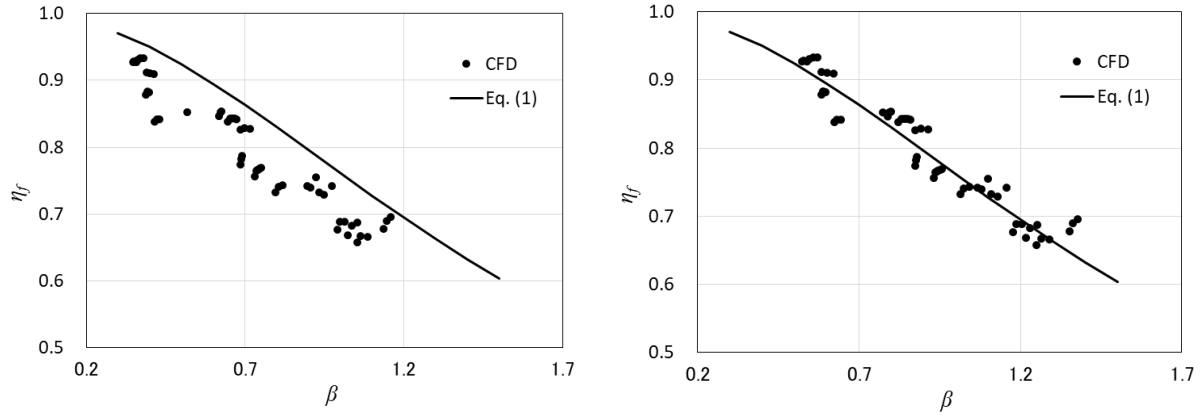

(a) β from equation (2) **(b)** β from equation (4)

Figure 2: Calculation results of fin efficiency

4. Air side heat transfer coefficient and pressure drop under dry conditions

For the flow between the fins of the heat exchanger, the air side heat transfer characteristic was summarized as a function of $Re \cdot Pr \cdot De_c / (Lp \cdot NR)$ using the representative length De_c in many studies. Similarly, in relation to the air side pressure drop, the friction factor was summarized as a function of $Re \cdot De_c / (Lp \cdot NR)$. In this study, the air side heat transfer characteristics and the friction factor are arranged using the same method as mentioned above. Here, Reynolds number Re is given as $Re = u_{ac} \cdot De_c / \nu$ using representative air velocity u_{ac}.

4.1 Representative air velocity and length

In the flat tube heat exchanger, the representative air velocity u_{ac} is defined as the following equation.

$$u_{ac} = \frac{Dp \cdot Lp \cdot Fp}{(Fp - t_f) \cdot \left\{ Dp \cdot Lp - \left(\frac{\pi \cdot d_{cS}^2}{4} + (d_{cL} - d_{cS}) \cdot d_{cS} \right) \right\}} \cdot u_{af} \tag{7}$$

The representative length De_c is defined as following equation in correspondence with the representative air velocity u_{ac}.

$$De_c = \frac{4 \cdot (Fp - t_f) \cdot \left\{ Dp \cdot Lp - \frac{\pi \cdot d_{cS}^2}{4} - (d_{cL} - d_{cS}) \cdot d_{cS} \right\}}{2 \cdot \left(Dp \cdot Lp - \frac{\pi \cdot d_{cS}^2}{4} - (d_{cL} - d_{cS}) \cdot d_{cS} \right) + \{\pi \cdot d_{cS} + 2 \cdot (d_{cL} - d_{cS})\} \cdot (Fp - t_f)} \quad (8)$$

4.2 Calculation results of the air side heat transfer coefficient and the pressure drop

In order to create a non-dimensional equation for the flat tube heat exchanger, the air side heat transfer and pressure drop characteristics were calculated by numerical analysis, in the range of parameters shown in Table 2. From the numerical analysis results of the external heat transfer coefficient h_o and calculation results of the fin efficiency by equation (4), the air side heat transfer coefficient h_a was calculated by the following equation.

$$h_o = \left(\frac{A_p + \eta_f \cdot A_f}{A_o} \right) h_a \quad (9)$$

The average Nusselt number *Nu* was calculated by the following equation.

$$Nu = \frac{h_a \cdot De_c}{\lambda_a} \quad (10)$$

From the numerical analysis results of the air side pressure drop characteristics, the friction factor *f* was calculated by the following equation.

$$f = \frac{De_c \cdot \Delta P_a}{2 \cdot Lp \cdot N_R \cdot \rho_a \cdot u_{ac}^2} \quad (11)$$

Table 2: Range of calculation parameter

Fin Pattern	$Dp - d_{cS}$	$Lp - d_{cL}$	Fin Pitch	Row Number	Reynolds Number
			FP	*NR*	*Re*
	mm	mm	mm	-	-
Flat	7.5～19.5	5～8	1.6	2	≦900

Figures 3 and 4 show the average Nusselt number *Nu* and the friction factor *f* calculated by equation (10) and equation (11) based on the numerical analysis results. Based on this result, the following non-dimensional equation was created. Figures 3 and 4 also show the calculation results of the average Nusselt number *Nu* and the friction factor *f* by the non-dimensional equations.

$$Nu = 3.48 \cdot \{Re \cdot Pr \cdot De_c / (Lp \cdot N_R)\}^{0.272} \quad (12)$$

$$f \cdot \frac{Lp}{De_c} = 0.14 + 23.3 \cdot \{Re \cdot De_c / (Lp \cdot N_R)\}^{-0.934} \quad (13)$$

The average Nusselt number *Nu* calculated by equation (12) and the friction factor *f* calculated by equation (13) are ± 11% and ± 6%, respectively, with the numerical analysis results, which were in good agreement. Therefore, in the case of the flat tube heat exchanger, as in the case of the circular tube heat exchanger, the air side heat transfer characteristic can be summarized as a function of $Re \cdot Pr \cdot De_c / (Lp \cdot NR)$, and the friction factor can be summarized as a function of $Re \cdot De_c / (Lp \cdot NR)$.

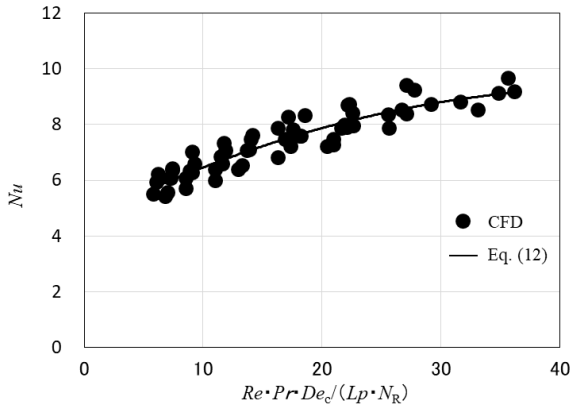

Figure 3: Calculation results of equation (12)

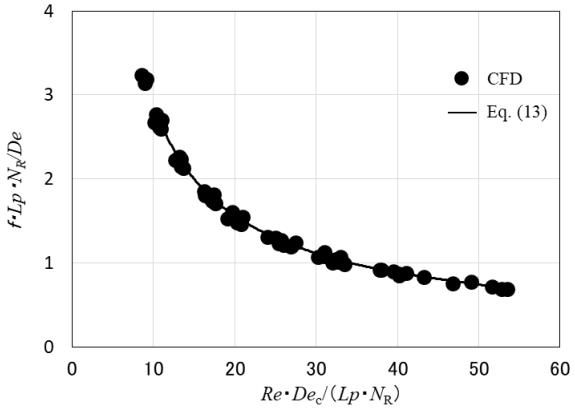

Figure 4: Calculation results of equation (13)

4.3 Effect of Reynolds number *Re*

Figure 5 shows the relationship between the Colburn's *j*-factor given by equation (14), the friction loss coefficient *f* and the Reynolds number *Re*. Here, λ_a is the thermal conductivity of the air. It is known that characteristics of *j* and *f* are transition near *Re* = 400 in the heat exchanger using a circular tube (Seshimo *et al*., 1987) (Kondou *et al*., 2006). On the other hand, the calculation results of the flat tube heat exchanger didn't have a transition. This is because the change of a flow field in the downstream area of a flat tube was small, due to small projected area of a flat tube in the direction of airflow.

$$j = \frac{Nu}{Re \cdot Pr^{1/3}} = \left(\frac{h_a \cdot De_c}{\lambda_a}\right) \cdot \frac{1}{Re \cdot Pr^{1/3}} \tag{14}$$

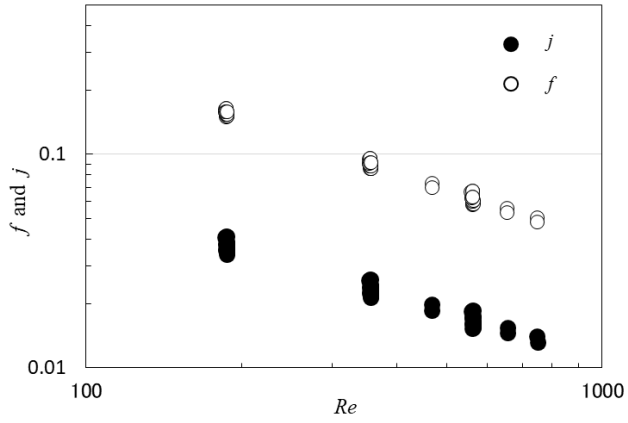

Figure 5: Dimensionless arrangements for the plane fins

4.4 Comparison between the calculation result and experimental result

In order to verify the accuracy of the non-dimensional equation, we measured the external heat transfer coefficient and the air side pressure drop. The method of the experiment was a general approach (Ishibashi *et al*., 2003), which measures the external heat transfer coefficient by placing a 300 x 300 mm heat exchanger in a wind tunnel, flowing the water with inlet temperature of 50℃ into the tubes, and the air with inlet temperature of 20℃ into the wind tunnel. Figure 6 shows the fin shape of the heat exchanger used in the measurement. Based on the measurement results, the following non-dimensional equation was newly created using the same simplification method as equation (12) and equation (13).

$$Nu = 3.39 \cdot \{Re \cdot Pr \cdot De_c/(Lp \cdot N_R)\}^{0.381} \tag{15}$$

$$f \cdot \frac{Lp}{De_c} = 0.19 + 16.5 \cdot \{Re \cdot De_c/(Lp \cdot N_R)\}^{-0.751} \tag{16}$$

Figures 7 shows the external heat transfer coefficient and the air side pressure drop calculated from equation (4), (9), (10), (15) and equation (11) and (16), and the measurement results. The external heat transfer coefficient according to equation (15) and the air side pressure drop according to equation (16) were ± 2% and ± 4%, respectively, with the measured results, which were in good agreement.

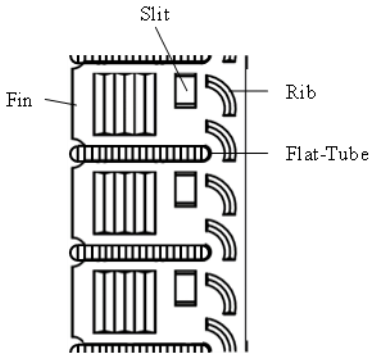

Figure 6: Specification of fin

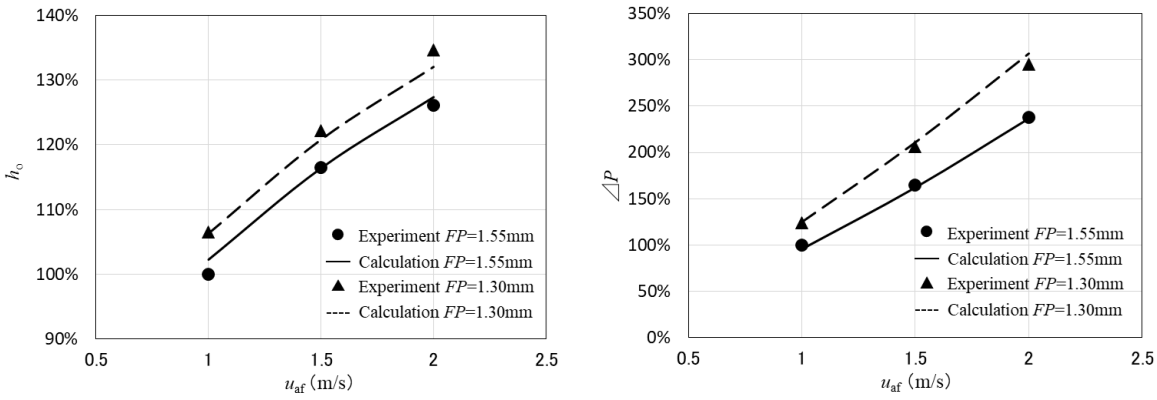

(a) Heat transfer Coefficient **(b)** Pressure drop

Figure 7: Comparison of measurement and calculation

5. Estimation of condensed water film thickness under wet conditions

Under wet conditions, the effect of condensed water on the air side pressure drop of the heat exchanger can' t be ignored because the condensed water covers the entire surface of fins. In this study, as shown in Figure 8, we quantified the water film thickness δ_P around the tube assuming that the water film thickness δ_F on the fin surface and the water film thickness δ_P around the tube are uniform over the entire heat exchanger. Here, the water film thickness δ_F on the fin surface is calculated by the equation of the falling liquid film (Brauer, 1956), and the water film thickness δ_P around the tube was determined so that the experimental results of the air side pressure drop matches the calculation results of the air side pressure drop obtained from equation (15). Figure 9 shows the calculation results of the water film thickness δ_P around the flat tube in the heat exchanger (with/without the slit in Figure 6), and the water film thickness δ_P around the tube calculated by Seshimo et al. (1988) based on the equation of the falling liquid film (Brauer, 1956) and the experimental results of the circular tube heat exchanger. In the flat tube heat exchanger, when there was no slit, δ_P was about 0.8-1.4mm, which was larger than that of the circular tube heat exchanger. This is because a large condensed water film was generated at the lower part of the flat tube. On the other hand, when there was the slit, δ_P was about 0.2-0.5mm, which was smaller than that of the circular tube heat exchanger. This is because the condensed water film at the lower part of the flat tube became smaller due to the water introduction effect of the slit (Nakamura *et al*., 2017).

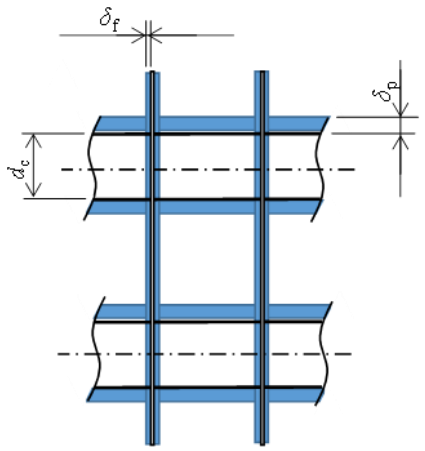

Figure 8: Specification of condensed water film thickness

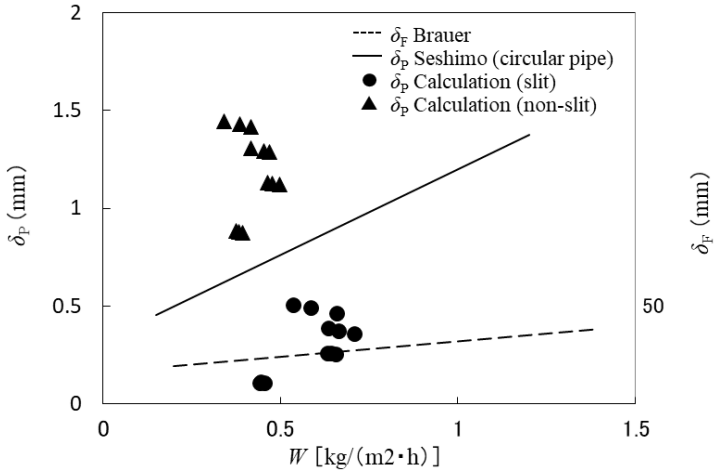

Figure 9: Effect of slit on condensed water film thickness

6. CONCLUSIONS

The calculation results, using a new fin efficiency equation with corrections in the row pitch direction and the column pitch direction, agree well with the numerical analysis results taking into account the air side local heat transfer coefficient. In addition, the calculation results, using non-dimensional equations for the air side heat transfer coefficient and the air side pressure drop under dry conditions in conventional form, and a new fin efficiency equation, agree well with the numerical analysis results and the measurement results. Furthermore, in wet conditions, it is suggested that the existence of the slit has a significant effect on the water film thickness around the pipe back-calculated from the measurement results and the non-dimensional equation.

NOMENCLATURE

d_{oS}	short side length of flat tube	(mm)
d_{oL}	long side length of flat tube	(mm)
d_{cS}	short side length of fin collar	(mm)
d_{cL}	long side length of fin collar	(mm)
t_f	thickness of fin	(mm)
Fp	fin pitch	(mm)
Dp	pipe pitch in the longitudinal direction of fins	(mm)
Lp	pipe pitch in the direction of airflow	(mm)
L_1	height of heat exchanger	(mm)
L_2	depth of heat exchanger	(mm)
EL	width of heat exchanger	(mm)
NR	row number of heat exchanger	(–)
A_p	outer tube surface area	(m^2)
A_f	fin surface area	(m^2)
De_c	representative length	(m)
λ_f	thermal conductivity of fin	($W \cdot m^{-1} \cdot K^{-1}$)
λ_a	thermal conductivity of air	($W \cdot m^{-1} \cdot K^{-1}$)
ρ_a	density of air	($kg \cdot m^{-3}$)
u_{af}	frontal air velocity	($m \cdot s^{-1}$)
u_{ac}	representative air velocity	($m \cdot s^{-1}$)
η_f	fin efficiency	(–)
Nu	Nusselt number	(–)
Re	Reynolds number	(–)
Pr	Prandtl number	(–)
h_a	air side heat transfer coefficient	($W \cdot m^{-2} \cdot K^{-1}$)
h_o	external heat transfer coefficient	($W \cdot m^{-2} \cdot K^{-1}$)
ΔP_a	air side pressure drop	(Pa)
j	Colburn's j-factor	(–)
f	friction factor	(–)
δ_F	condensed water film thickness on fin	(mm)
δ_P	condensed water film thickness on pipe	(mm)
W	weight of condensed water	($kg \cdot m^{-2} \cdot h^{-1}$)

REFERENCES

Y. Seshimo, *et al*: *Trans. Jpn. Soc. Mech. Eng.Ser.B*, Vol.53, No.486 587-592 (1987). (in Japanese)
C. Kondou, *et al*: *Proc. 2006 JSRAE Annual Conference*, JSRAE, (2006), pp. 437-446. (in Japanese)
K. Fujikake, "Miniaturization of heat exchanger by expansion heat transfer surface", JSME Seminer textbook, Vol.506, 67-82 (1980). (in Japanese)
A.Ishibashi *et.al*. :*40th National Heat Transfer Symposium of Japan*, 491(2003). (in Japanese)
Brauer H., VDI-Forsch, 22,457(1956).
Y. Seshimo, *et al*:*Trans. Jpn. Soc. Mech. Eng.Ser.B*, Vol.54, No.499 716-721 (1988). (in Japanese)
S. Nakamura, *et al*: *Proc. 2017 JSRAE Annual Conference*, JSRAE, (2017), A343. (in Japanese)